Journal of Catalysis **208,** 260–269 (2002)
doi:10.1006/jcat.2002.3540

Carbonaceous Deposition on Mo/HMCM-22 Catalysts for Methane Aromatization: A TP Technique Investigation

Ding Ma, Dezheng Wang, Lingling Su, Yuying Shu, Yide Xu, and Xinhe Bao[1]

State Key Laboratory of Catalysis, Dalian Institute of Chemical Physics, Chinese Academy of Sciences, 457 Zhongshan Road, P.O. Box 110, Dalian 116023, China

Received June 7, 2001; revised January 3, 2002; accepted January 3, 2002

TPO (temperature-programmed oxidation), TPSR (temperature-programmed surface reaction), and TPH (temperature-programmed hydrogenation) techniques are used to investigate carbonaceous deposition on Mo/HMCM-22 catalysts for methane aromatization. Different carbonaceous species and their amounts are distinguished. There are at least three kinds of cokes: carbidic carbon in molybdenum carbide, molybdenum-associated coke, and aromatic-type cokes on acid sites. It is suggested that the aromatic-type cokes on Brønsted acid sites are responsible for catalyst deactivation. Catalytic activity can be restored after temperature-programmed hydrogenation. © 2002 Elsevier Science (USA)

INTRODUCTION

Microporous materials, especially zeolites, are used frequently as supports for metal and metal oxide catalysts (1), but these materials can also be more than just the supports needed for high dispersion (1–3). The channel structure and the acidity or basicity of these materials can play a role in the activation of reactant or the transformation of intermediates, resulting in a bifunctional catalyst. Mo-based zeolite catalysts are highly efficient catalysts for methane aromatization (4–11). The molybdenum species is the active center for methane activation, whereas surface acid sites, especially Brønsted acid sites, are responsible for the aromatization of the intermediates. During the reaction, carbonaceous deposition occurs, which has been reported as responsible for the short lifetimes of these catalysts. Three kinds of carbonaceous deposits have been distinguished by angle-resolved XPS by Lunsford and coworkers (12), who suggested that a sp-type coke on the external surface of the zeolite gradually covers Mo centers and the zeolite surface and is responsible for the deactivation of the catalysts.

Recently it has been reported that Mo/HMCM-22 are highly selective catalysts for benzene formation (10, 11), with a higher yield toward benzene compared with Mo/HZSM-5 catalyst. A synergistic effect between the molybdenum species and the zeolite of this sort of catalyst has been shown to exist (13). It is generally accepted that temperature-programming methods, especially temperature-programming oxidation (TPO), are sensitive techniques for the investigation of coke deposition on catalysts (14–19). The type, location, and amount of carbonaceous deposits can be determined. In this paper, TP techniques are used to elucidate the carbonaceous deposition process on Mo/HMCM-22 catalysts during methane aromatization. The different types of coke that are generated on different sites, molybdenum and zeolite, and the effect of coke on catalytic performance are also clarified.

EXPERIMENTAL

Catalysts

MCM-22 zeolite (Si/Al = 15) was synthesized according to the procedures described in Ref. (20), using hexamethyleneimine (HMI) as the directing agent. Mo/HMCM-22 catalysts containing 2–10% Mo were prepared by impregnating 10 g of HMCM-22 powder with 20 ml of aqueous solution containing the desired amount of ammonium heptamolybdate (AHM). After drying at room temperature for 12 h, further drying at 373 K for 8 h, and calcination in air at 773 K for 4 h, the samples were crushed and sieved to 20–60 mesh granules. These Mo/HMCM-22 catalysts with different Mo loading are denoted xMo/HMCM-22, where x is the nominal Mo content in weight percent. The actual molybdenum contents, which are determined by elemental analysis, are sometimes used (13), and this is noted where relevant. The preparation of 6% Mo/TiO_2 catalysts was carried out using a similar procedure, and the catalysts are denoted as 6Mo/TiO_2.

Reaction and TP Experiments

The reaction was carried out in a 6.2-mm i.d. quartz tubular fixed-bed reactor. The products were analyzed by an online gas chromatograph (Shimadzu GC-9A) equipped with a flame ionization detector and a OV-101 6201 column,

[1] To whom correspondence should be addressed. Fax: 0086-411-4694447. E-mail: xhbao@dicp.ac.cn.

0021-9517/02 $35.00

and a thermal conductivity detector and a HayeSep-D column (9).

The temperature-programming apparatus was described in our previous paper (11). Gas flows were controlled by mass flow controllers (Jian Zhong, D08-4A/ZM). Three four-port valves and a six-port valve were used to smoothly switch the gas entering the reactor between four kinds of gases. Reaction products and desorption products were analyzed by an online quadruple mass spectrometer (Balzers, QMS 200) equipped with a computer interface.

The reactor was charged with 150 mg of catalyst. For TPSR, the catalyst was first heated under a He stream (30 ml/min) to 873 K (10 K/min) and kept at this temperature for 40 min to remove adsorbed water. After cooling to room temperature (RT), the sample was flushed with methane (99.99%, 3.75 ml/min) for 1 h. Then, TPSR was initiated from 293 to 973 K at a heating rate of 5 K/min and kept at 973 K for 1.3 h, at which point the reaction reached a relatively stable stage. Product gases leaving the reactor were analyzed by the mass spectrometer through a capillary. During the temperature ramp, m/e intensities at 2 (H_2), 15, 16 (CH_4), 18 (H_2O), 28 (CO), 44 (CO_2), and 78 (C_6H_6) were measured as a function of temperature. TPO was performed after the catalyst had been used for different times on stream (using a fresh sample each time). After the reaction the catalyst was quickly cooled in the reaction atmosphere and then flushed with a 10% O_2/He mixture (20 ml/min) at RT for 1 h. The temperature was raised from 303 to 1023 K at a rate of 8 K/min during which the m/e intensities for 44 (CO_2), 28 (CO), and 18 (H_2O) were recorded. The CO_2, CO signals were calibrated by burning different weights of $Cu(CO_3) \cdot Cu(OH)_2$. CO_2 contributes a fragment to the signal at $m/e = 28$, and this was subtracted from the total intensity at $m/e = 28$ to get the amount of CO. Also, since CO and CO_2 showed similar curve shapes, the amount of CO was added to that of CO_2 to simplify the analysis, which was performed in terms of carbon oxides. In some TPO experiments, the deactivated sample was temperature-programmed hydrogenated in pure H_2 (15 ml/min) from 293 to 1095 K at a heating rate of 5 K/min and further hydrogenated at 1095 K for 30 min to remove specific kinds of carbonaceous deposit.

All gases used were UHV grade.

Deconvolution

TPO results were simulated using a kinetics expression similar to Querini and Fung [17].

$$\partial C/\partial t + V\,\partial C/\partial \xi = \sum A_i \cdot e^{-Eai/RT} \cdot C_{i0}^{ni} \cdot (1 - X_i)^{ni} \cdot P_{O_2}^{mi},$$

where C_{i0} is the initial concentration of coke, A_i is the preexponential factor, E_{ai} is the activation energy, n_i is the reaction order of coke, P_{O_2} is the partial pressure of oxygen, m_i is the oxygen reaction order [which is taken as 1 following Querini and Fung (17)], and V is the flow rate. Different types of coke species, denoted by subscript i, were assumed and the fit of simulated TPO peaks to experimental results was used to determine the number of these types and their kinetic parameters. The reactor equations were integrated numerically using the upwind scheme algorithm for solving partial differential equations (21).

RESULTS AND DISCUSSION

TPO Profiles of the Various Catalysts

Catalytic activities of the catalysts used in this study are listed in Table 1. No benzene formation was observed on HMCM-22 and 6Mo/TiO_2 catalysts. This is due to the absence of molybdenum and Brønsted acidity, respectively. Dissociated methane on both these catalysts are mainly transformed into coke. 6Mo/TiO_2 had a longer lifetime for the activation of methane. All the Mo/HMCM-22 catalysts have methane aromatization activity, with 6Mo/HMCM-22 giving the highest benzene yields. The benzene yields of these catalysts show a volcano-shaped curve, indicating the bifunctional nature of these catalysts. During impregnation and calcination of the catalyst, molybdenum migrates into the zeolitic channel of HMCM-22 and reacts with the Brønsted acid sites to form a monomer or dimer species (8, 9), with a stoichiometry that was reported as one molybdenum atom to one Brønsted acid site. Thus, with more molybdenum species, there will be fewer remaining Brønsted acid sites, and the best benzene yield results when these two sites have an optimal balance (13). There is an insufficient number of molybdenum species (the center for methane acitivation) in 2Mo/HMCM-22 and an insufficient number of Brønsted acid sites (the center for intermediate aromatization) in 10Mo/HMCM-22 for good aromatization activity, and they are poor catalysts for methane aromatization. A suitable ratio and synergy of molybdenum species and Brønsted acidity in 6Mo/HMCM-22 is responsible for its outstanding catalytic performances.

TABLE 1

Catalytic Performance of Various Catalysts

Catalyst	C_{CH4}(%)	Selectivity of main products (%)		
		C_6H_6	$C_{10}H_8$	Coke
6Mo/TiO_2[a]	1.8	—	—	≈100
HMCM-22[a]	0.5	—	—	≈80
2Mo/HMCM-22[a]	6.4	57.5	7.3	27.9
6Mo/HMCM-22[a]	10.4	71.0	5.1	17.9
10Mo/HMCM-22[a]	6.2	60.3	3.3	29.2
6Mo/HMCM-22[b]	8.5	74.7	4.7	14.1
6Mo/HMCM-22[c]	9.9	72.6	4.6	18.2

Note. The reaction was conducted at 973 K and SV = 1500 ml/g · h.

[a] data taken after 150-min reaction.

[b] After 6-h reaction.

[c] After 6-reaction and a TPH treatment.

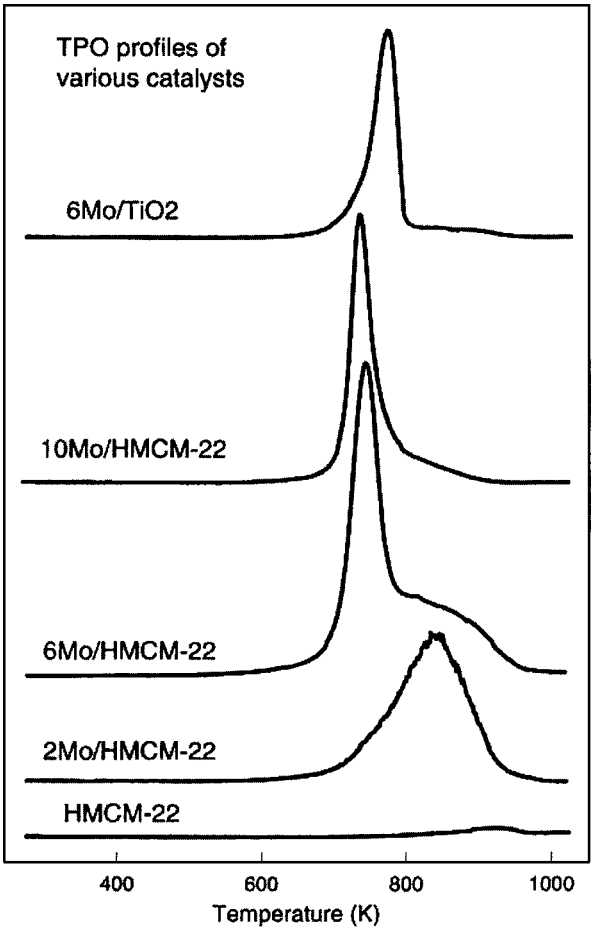

FIG. 1. TPO profiles of different catalysts. The catalysts first underwent methane aromatization for 3 h (973 K; methane flow rate, 3.75 ml/min), then were quenched to RT in a methane atmosphere. After flushing with a 10% O_2/He mixture (20 ml/min) at RT for 1 h, the TPO experiment was begun from 303 to 1023 K at a heating rate of 8 K/min.

The TPO profiles of various catalysts after 3 h on stream are shown in Fig. 1. After a 3-h reaction there is almost no coke on HMCM-22. The TPO profile of 6Mo/HMCM-22 consists of a sharp peak at 743 K and a broad shoulder on the high-temperature side. A similar double-peak feature from molybdenum-loaded ZSM-5 catalysts had been reported by Ichikawa and coworkers (22), and verified by other workers (23). Ichikawa and coworkers attributed the high-temperature peak (higher than 773 K) to irreversible or inert coke, whereas a more reactive coke (lower than 673 K) is probably associated with Mo_2C. The high-temperature peak can be suppressed by the addition of small amounts of CO or CO_2 to the methane feed, which results in better stability as compared with using pure methane as the feed gas (22). These kinds of TPO peaks are typical of a bifunctional catalyst, especially of zeolite-supported metal catalysts, as has been reported by Sachtler and coworkers (14), with the first peak being due to coke oxidation catalyzed by the metal and the broad peak being due to thermally initiated coke oxidation of coked acid sites. XPS and EXAFS experiments under working conditions have proved that molybdenum carbide is formed during the reaction process (5–7, 11, 24, 25). Two additional carbon species, other than carbidic-like C, have been observed by angle-resolved XPS (12), with the former being attributed to adventitious or graphitic-like C in the zeolite channel system and the latter to a pregraphitic type of carbon. Based on these reports, we have assigned the low-temperature peak in the present work to coke associated with molybdenum, and the high-temperature peak to carbonaceous deposits on acid sites, mostly Brønsted acid sites in the zeolite channels. If this hypothesis is correct, catalysts without strong acid sites will not give the peak related to the Brønsted acid sites. The absence of a high-temperature peak in the TPO profile of $6Mo/TiO_2$ (which does not have strong Brønsted acid sites) supports this assignment that the high-temperature peak is associated with Brønsted acidity. Since there are no Brønsted sites in $6Mo/TiO_2$, no benzene formation or acid-related aromatization would be observed, and no acid-associated carbonaceous deposition would be observed. The origin of the low-temperature peak is discussed in the following section in detail. The relatively large amounts of carbonaceous deposit (with $C/Mo > 3$) in the first peak is due to a special feature of molybdenum (as compared with other metal, such as Co), namely, it can continuously dissociate methane even when multiple layers of coke cover its surface (11).

It has been reported that methane activation occurs on the molybdenum species, while the transformation of intermediates occurs on the acid sites (5–9, 26), with the commonly proposed intermediate being ethene (4, 5). Here, it is pointed out that only a very small amount of ethene was detected besides the vast amount of carbonaceous deposits, in TPSR experiments following the formation of molybdenum carbide. Thus, it is hard to draw an unambiguous conclusion at present as to which species is the intermediate in this reaction because the current results indicate that gas-phase ethene is not responsible for the production of aromatics. Meriaudeau *et al.* [27] had made a similar suggestion on the basis of a higher activity on Mo/H–zeolite as compared to H–zeolite for ethene or acetylene conversion to benzene and questioned the correctness of those simplified intermediates [ethane (4, 5) or acetylene (28)] suggested previously. In the methane conversion, the initial C–H bond rupture forms adsorbed CH_x species (which account for the carbonaceous depositions) on the metal surface, and coupling and conversion to intermediates or products of higher molecular weight take place on adjacent sites. A possibility is that the intermediate is not desorbed into the gas phase but is an adsorbed species (C_xH_y) which stays on the catalyst surface, i.e., a living coke (surface-active carbon species) (22) or a carbon pool exists (29).

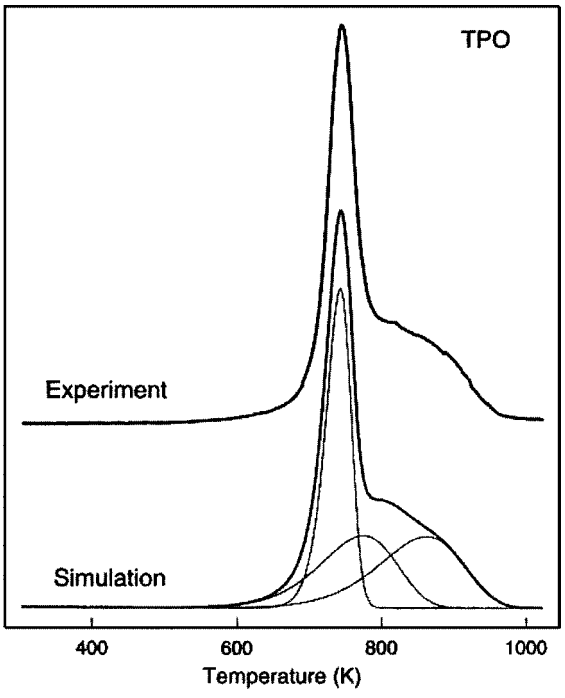

FIG. 2. The TPO profile of 6Mo/HMCM-22 after 3 h time on stream (upper), and a simulated TPO profile showing the deconvolution of the peaks.

However, the identification of this species needs advanced spectroscopic techniques, such as pulse-quench NMR spectroscopy (30, 31), which can detect *in situ* carbonaceous deposition in high-temperature catalytic reactions.

The TPO profiles of 2Mo/HMCM-22 and 10Mo/HMCM-22 give quite different pictures: the former has a broad peak centered at 837 K while the latter has a sharp peak at 735 K. Nevertheless, these superficially complicated TPO spectra are in good agreement with the bifunctional nature of these Mo/zeolite catalysts, which can be explained as follow. 2Mo, 6Mo, and 10Mo/HMCM-22 catalysts are in an ascending sequence in molybdenum content but a descending sequence in the number of Brønsted acid sites (3.0, 1.1, and 0.7 per u.c.) due to the occupation of Brønsted sites by molybdenum (13). By assigning the high-temperature TPO peak to carbonaceous deposits on acid sites and the low-temperature peak to those associated with molybdenum, it can be seen that 2Mo/HMCM-22, which has the lowest molybdenum content and the highest number of Brønsted acid sites, will have a large peak in the high-temperature (related to acid sites) region, whereas 10Mo/HMCM-22 will have the reverse spectrum (a large peak in the low-temperature region related to molybdenum). At the same time, the double-peak structure can be clearly resolved with a catalyst that possesses both a moderate molybdenum content and a moderate number of Brønsted sites, e.g., 6Mo/HMCM-22. Actually, it may be noted that the TPO profiles of 2Mo/HMCM-22 and 10M/HMCM-22 are asymmetric; the former has a low-temperature part and the latter has a high-temperature shoulder. This indicates that both catalysts have at least two kinds of carbonaceous deposits (on molybdenum and on acid sites), while which kind of carbonaceous deposit is the dominant one in TPO profiles is governed by the molybdenum content and the balance between molybdenum and Brønsted acid sites. Interestingly, one can also note that there is no linear dependence of the low- or high-temperature peak on the molybdenum content or the number of Brønsted acid sites, indicating the complex nature of the mechanism of coke formation.

At the same time, it is also worthwhile to point out that the catalyst with the best catalytic performance (methane conversion, benzene yield, and lifetime) is not the one with the lowest coke content. In fact, it has the highest coke content (the total coke contents of 2Mo, 6Mo, and 10Mo/HMCM-22 are 3.85, 4.62, and 1.95 mmol/g, respectively). This fact implies that not all cokes are responsible for deactivation of the catalysts.

The TPO spectra were deconvoluted by a reaction scheme similar to that used by Querini and Fung (17), but without a pseudo-steady-state assumption. The results are shown in Fig. 2 and Table 2. Due to the overlap of the oxidation peak of acid-related coke with that of the molybdenum-associated one, it is difficult to extract the exact high-temperature band shape from the TPO experiment alone. In the present case, a shape similar to that of the oxidation peak of coke on HZSM-5 (15) is used to deconvolute the high-temperature peak. A satisfactory fit can be achieved only when at least three peaks are used, with the high-temperature peak being composed of two peaks. The peak indices i in Table 2 refer to the corresponding peaks marked in Fig. 2. Peak $i = 1$ is the above-mentioned low-temperature peak while the next two peaks, $i = 2$ and $i = 3$, are in the region of the high-temperature peak associated with Brønsted acid sites. Peak 1 has an activation energy of 292 kJ/mol while the other two have values around 100 kJ/mol. The similar values of the kinetic parameters of these latter two peaks suggest that they are probably from carbonaceous deposits that are identical in nature, i.e., the latter two peaks are due to aromatic coke on different kinds of acid sites. By ^{27}Al MAS NMR experiment, it is

TABLE 2

Parameters Estimated from the TPO Profiles of 6Mo/HMCM-22 after 3 h time on Stream Using Eq. [1][a]

I	E_{ai} (kJ/mol)	C_{i0} (mmol/g)	n_i
1	292.1	1.92	1.30
2	90.1	1.29	0.98
3	101.2	1.41	1.00

[a] A_i has no statistical significance.

apparently that there are at least two 4-coordinated Al peaks for MCM-22 zeolite, different from that of HZSM-5, which just has one band (32). These two aluminum peaks are attributed to two sets of framework tetrahedral sites, differentiated by their location in small and large atom rings, by different pores systems (32), or by different T sites (33, 34). At the same time, different kinds of Brønsted acid sites have been shown to exist by IR (35) and benzene-TPD (15), among other methods. Therefore, it is reasonable to assume that the carbonaceous species will deposit on these two different Brønsted acid sites, thus leading to the two aromatic coke peaks. Meanwhile, in addition to the fact that there is only one kind of aromatic peak, at around 1600 cm^{-1} in UV-Raman spectrum of deactivated 6Mo/MCM-22 catalyst (34), the variation of the two aromatic cokes with respect to time on stream (see Fig. 5; they seems to be almost identical) seems not to support the view that there are indeed two forms of aromatic coke. However, the absence of the other aromtic-type peak in the UV-Raman experiment may also result from the relatively poor resolution of the UV-Raman instrument. This problem is open for further investigation. Probably, the application of a spectroscopic method such as ^{13}C-enriched ^{13}C MAS NMR experiments (31) may provide an answer. The relatively larger coke reaction order of peak 1 (larger than 1) suggests that a distribution of different coke types exists or that the structure of the coke changes during the heating (19). We believe the first possibility is more reasonable since we cannot distinguish carbidic carbon from coke closely associated with molybdenum carbide in the present case; this is further discussed in the following section. The activation energy of the low-temperature peak is about two times higher than the high-temperature peaks. A possible explanation is that the combustion of the coke of the low-temperature peak is composed of several reaction steps (such as is initiated by carbidic carbon in MoC_x, where the combustion of carbidic carbon is autocatalytic) and the much higher activation energy measured is not an intrinsic activation energy but an apparent activation energy. The preexponential factors have no statistical significance and are not discussed. C_{i0} is an important bit of information obtained. It gives the number of different coke species in the catalysts and is used in the following section.

TPO Profiles of 6Mo/HMCM-22 Catalysts after Different Times on Stream

6Mo/HMCM-22 is the best catalyst for this reaction, so the following investigation focuses on 6Mo/HMCM-22. A TPSR experiment of 6Mo/HMCM-22 under conditions identical to the catalytic reaction, which is different from our former study (11) (where the temperature was increased smoothly from 293 to 1095 K), is presented in Fig. 3. As shown in Fig. 3, when the temperature is near 900 K, a reaction between molybdenum species and methane occurred, with the formation of CO_2, CO, H_2O, and H_2. This stopped about 15 min after reaching 973 K. At the same time, benzene formation is observed. The formation rate of benzene increased with time on stream, together with a relatively constant H_2 formation, and does not reach a stable value in this experimental range. This stage in methane aromatization is the so-called induction period of this reaction.

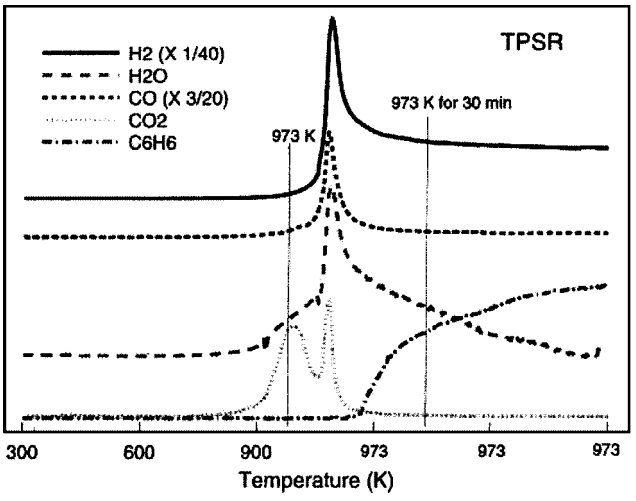

FIG. 3. TPSR profiles of 6Mo/HMCM-22 after a procedure similar to the catalytic reaction. Before the TPSR the catalyst was dried in He flow (30 ml/min) at 873 K for 40 min. After cooling to RT, the catalyst was swept by methane (99.99%, 3.75 ml/min) at the same temperature for 1 h. Then the temperature was raised from 293 to 973 K at a heating rate of 5 K/min and kept at 973 K for 1.3 h. Benzene formation was observed about 15 min after the temperature reached 973 K.

TPO profiles of 6Mo/HMCM-22 catalysts with different times on stream are shown in Fig. 4. The lines of those after 10- and 20-min reaction are enlarged and placed in the upper left corner of the figure. The TPO of 6Mo/HMCM-22 after 20 min time on stream presents a picture similar to that after 3 h: there is a low temperature peak at 694 K due to a carbonaceous deposit associated with molybdenum species and a high-temperature peak associated with Brønsted sites which is a shoulder of the former. Similar behavior has been observed in the water-formation curve, indicating the existence of hydrogen in both the molybdenum-associated and the aromatic carbonaceous depositions. Here we cannot attribute the low-temperature peak to carbidic carbon in Mo_2C, because after 6 h time on stream, $C_{\text{first peak}}/\text{Mo} \gg 1$ and is far different from the stoichiometry of Mo_2C. However, EXAFS, XPS, and XANES experiments (5–7, 24, 25) have shown that molybdenum carbide is formed after the induction period. TPO of the catalyst after 10 min time on stream shows a dramatic change: there are also two oxidation peaks, but the peak temperatures are totally different. The high-temperature peak (694 K) has a peak center identical to the

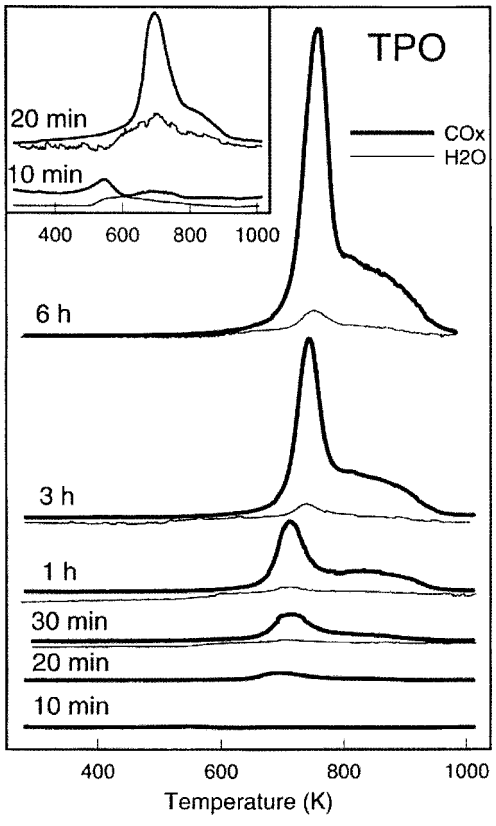

FIG. 4. TPO profiles (in 20 ml/min 10% O_2/He mixture; heating rate, 8 K/min) of 6Mo/HMCM-22 catalysts with different times on stream (3.75 ml/min methane flow). (upper left corner) The spectra after 10 and 20 min, enlarged. In enlargement, a distinct CO_x peak at about 550 K can be observed in the profile from 6Mo/HMCM-22 after the 10-min reaction.

low-temperature peak (molybdenum associated) in the TPO profiles of the catalysts after a 20-min reaction, whereas the other peak, which is not seen in the other TPO profiles, appeared at around 550 K. It should be noted from Fig. 3 that benzene formation had occurred beginning at about 15 min after the temperature reached 973 K; consequently some undesorbed aromatic (C_xH_y) could be left in the zeolite channels. However, aromatic-type coke should not be present in the TPO spectra before 15 min time on stream. In fact, we did not observe this kind of coke in the TPO of the catalyst after a 10-min reaction (there is no peak with temperature higher than 694 K), strongly supporting our assignment of the high-temperature peak: an aromatic-type acid-related carbonaceous deposit. On the other hand, a new peak at 550 K, which was not observed in other TPO profiles, appeared. This is just the carbidic carbon in molybdenum carbide (12). It is interesting to note that a water-formation peak beginning from 520 K also appeared in the TPO experiment of a catalyst after a 10-min reaction. This fact reveals the existence of hydrogen in the molybdenum carbide. Oyama and coworkers (41) carried out a TPD in He of a $Mo_2C/A1_2O_3$ catalyst and found that some methane was produced at 723 K, and the authors stated that it may have been due to dissolved hydrogen or chemisorbed hydrogen. We believe that a similar property of molybdenum carbide accounts for the present observation.

Our previous work (9) shows that during the impregnation and calcination process of Mo/zeolite catalyst part of the molybdenum will diffuse into the lattice channel of zeolite and anchor on the Brønsted aluminum, whereas the others remain on the external surface as molybdenum clusters; this has been confirmed by ESR experiment. Thus, the oxidation peaks of two kinds of molybdenum carbide should be observed in the TPO of a catalyst after a 10-min reaction: one is from isolated Mo ions and the other is from molybdenum particles at the external surface of the zeolite. We believe the external molybdenum carbide particles have properties similar to the bulk molybdenum carbide. It is clear from Ref. (36) that the oxidation peak of bulk molybdenum carbide is at 725 K, very similar to the peak temperature of the high-temperature band in TPO of the catalyst after a 10-min reaction. Thus, it is reasonable to conclude that the oxidation peak of an external molybdenum carbide particle (around 725 K) will overlap with that of molybdenum-associated coke (around 700 K). The relatively large activation energy of the oxidation peak at around 710 K may result from the fact that it is the combustion processes of different kinds of carbonaceous species. After a longer time on stream, molybdenum carbide (both of isolated Mo ions and external Mo particles) would be covered by coke on its surface, and the carbidic carbon may not be directly exposed to oxygen. So although it is easily burnt off when there is no coke covering, after molybdenum carbide is fully covered by coke its oxidation peak will be buried in that of the coke covering its surface (molybdenum-associated coke). Thus only one peak below 800 K can be observed in a TPO profile. The calculated carbon content in 6Mo/HMCM-22 when all its molybdenum oxide is transformed to molybdenum carbide would be 1.88×10^{-4} mol/g (calculated from the actual molybdenum content from elemental analysis), while all the coke (carbidic and molybdenum associated) in the catalyst after a 10-min reaction is 3.03×10^{-5} mol/g, indicating that not all the molybdenum oxide has changed to molybdenum carbide at this time. For the catalyst after 30 min time on stream, the carbon of both the carbidic and molybdenum-associated peaks is 2.0×10^{-4} mol/g. The carbon amount quickly increased and is 1.15×10^{-3} mol/g after a 1-h reaction, where we believe a multilayered carbonaceous deposit must have formed on the molybdenum carbide surface. The peak temperature of the molybdenum-associated coke gradually increases with times on stream (from 694 to 758 K), indicating that the particle size of this kind of coke grows bigger with time on stream (17). A recent publication has also reported a three-peak structure in the TPO profiles of Mo/HZSM-5 catalysts (36), and

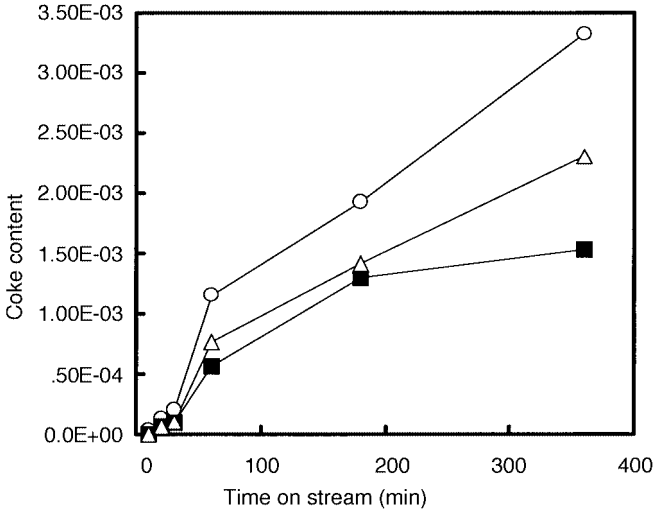

FIG. 5. Variation of the different kinds of cokes with different times on stream. ○, Molybdenum-associated coke; ■ and △, low-temperature and high-temperature aromatic-type cokes, respectively.

a relatively similar assignment was made to (i) carbidic carbon in MoCx, (ii) carbonaceous species within zeolite channels near Mo species, and (iii) carbon deposits distant from these Mo species. However, the authors did not indicate which kind of coke is deposited on acid sites; thus it is aromatic in nature.

The variation in the amount of different cokes with different times on stream is shown in Fig. 5. A similar trend is shown by the three kinds of coke: they all increased with time on stream and a comparatively sharp increase occurs between 30 min and 1 h, implying that the coke deposition in this period is unique. However, we cannot deduce the kind of coke responsible for catalyst deactivation from this figure. The increase in carbonaceous deposits is in accordance with the decrease of the BET surface areas of the catalyst with time on stream, i.e., after a 6-h reaction, the surface area of the catalyst decreased from around 400 to about 300 m^2/g. It is the result of channel blockage originating from the growing of the coke deposits (37). As determined from knowledge of the channel system of MCM-22 (38), the most likely location of channel blockage is the bottleneck of the 12-MR system—10-ring windows between the 12-ring supercages. Since molybdenum is located in the 12-MR system of MCM-22, (13) mainly in the supercages and not in the 10-ring window connecting the supercages, it is unlikely that a molybdenum-related coke would contribute much to the blockage of the 12-MR system. Nevertheless, the products (benzene, naphthalene, and other bulk aromatics) formed in the supercages (12 ring) have to pass the relatively smaller 10-ring window in their migration in and diffusion out of the channels, possibly leaving an aromatic-type coke on the acid sites of these windows with a significant role in the jamming of the zeolite channels.

As determined from the above discussion, there are at least three kinds of carbonaceous deposits on the catalysts: carbidic carbons (in isolated Mo ions or in external Mo particles), molybdenum-associated coke, and (possibly two kinds of) aromatic-type cokes on acid sites. While there is no benzene formation, the aromatic-type coke deposition associated with Brønsted acid sites does not occur, and carbidic carbon dominates the TPO spectrum. With longer reactions, coking on the acid sites occurs, and at the same time, molybdenum carbide gets covered with carbonaceous deposits which mask the carbidic carbon peak in TPO profiles. The longer the reaction time, the thicker the layer on the molybdenum carbide (cf. the increase in the area of the peak around 700 K in Fig. 4 with time on stream). However, a continual methane consumption is still observed, which has been reported in our previous paper as a special feature that molybdenum/molybdenum carbide catalysts possess (11). One of the reasons for deactivation of the catalyst is believed to be channel blockage by aromatic-type coke on Brønsted acid sites, which makes diffusion and migration of molecules difficult.

TP Hydrogenation and Subsequent TPO

After 6Mo/HMCM-22 underwent a methane aromatization reaction for 3 h, the catalyst was cooled quickly to room temperature in a methane flow. It was flushed by hydrogen at RT for 1 h; then a TPH experiment was begun, with heating from 293 to 1095 K at a heating rate of 5 K/min and keeping it at 1095 K for 30 min. Figure 6 shows the CH_4, C_2H_4,

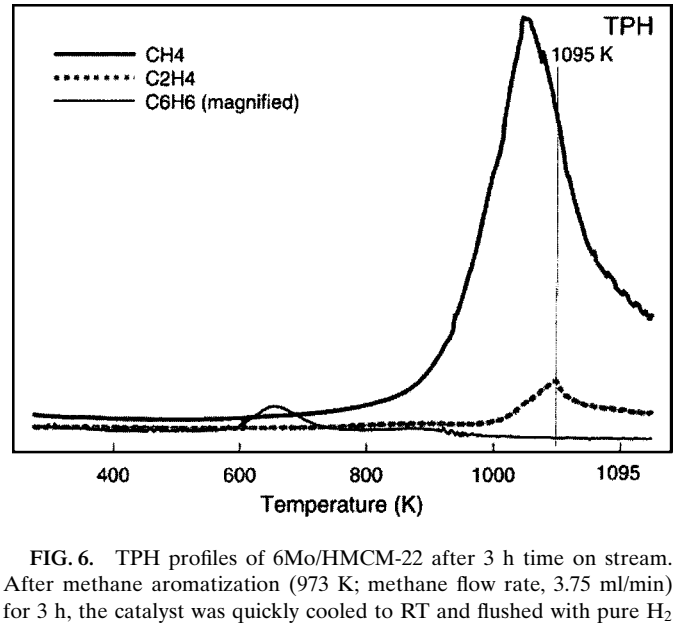

FIG. 6. TPH profiles of 6Mo/HMCM-22 after 3 h time on stream. After methane aromatization (973 K; methane flow rate, 3.75 ml/min) for 3 h, the catalyst was quickly cooled to RT and flushed with pure H_2 (15 ml/min) at RT for 1 h. The temperature was then raised from 293 to 1095 K at a heating rate of 5 K/min and kept at 1095 K for 30 min. The amount of benzene is extremely small, and the curve has been magnified many times.

and benzene responses obtained during TPH. Most of the cokes are transformed into methane during TPH, starting at about 700 K and with a peak maximum at 1047 K. A small amount of ethene formation is observed at relatively higher temperatures, but the peak maximum was not obtained because of the cessation of the temperature increase. Meanwhile, a trace amount of benzene formation was observed. This benzene may be due to its strong adsorption during the reaction or hydrogenation of CH_x deposited on the catalyst surface, as reported on other catalysts (39). Direct desorption in He after reaction was performed to rule out the first possibility. Although there was some benzene desorption, it was different from the line shape observed in TPH; but admittedly there are experimental difficulties with the mass spectrometer because of such low signal intensity. The differences in the peak centers and shapes of methane and ethene formation during temperature-programmed hydrogenation suggest that they are from two different mechanisms and may be from two different kinds of cokes. The TPH features of 6Mo/HMCM-22 catalysts with different times on stream are similar, with increasing peak intensity of methane and ethene with reaction time.

Figure 7 shows the TPO profiles of 6Mo/HMCM-22, 2Mo/HMCM-22, and 10Mo/HMCM-22 after different reaction times and a consequent TPH (this kind of TPO is termed HTPO). After hydrogenation, only 20% coke remained on 6Mo/HMCM-22 (after a 30-min reaction) as compared with the nonhydrogenated case. Both the molybdenum-associated and aromatic-type cokes were much decreased, whereas a new peak appeared at about 570 K. It is interesting to note that this peak also appears in the HTPO of 6Mo/HMCM-22 after longer reaction times and the HTPO of 10Mo/HMCM-22. In the latter case, the peak area is larger (by two times) than that of 6Mo/HMCM-22, whereas no peak was seen in the HTPO spectra of the low-molybdenum-content catalyst (2Mo/HMCM-22, which contains 1.1% molybdenum according to elemental analysis). This peak maximum is similar to the first peak during TPO of 6Mo/HMCM-22 after 10 min time on stream (see Fig. 4) and it does not appear in the TPO profile of 6Mo/HMCM-22 catalysts after a 30-min reaction. These observations suggest that this peak is directly related to molybdenum and, in fact, is from the carbidic carbon in molybdenum carbide. Although molybdenum carbide is covered by molybdenum-associated coke after 30 min time on stream, the carbonaceous deposits on its surface will be removed after hydrogenation, leading to the appearance of the carbidic carbon peak in HTPO experiments, again affirming our assumption of the carbidic carbon peak. For these HTPO experiments, the formation of water presents a broad band ranging from 400 to about 1000 K. This broad band may result from the overlap of the oxidation of hydrogen in the carbonaceous depositions and that of the hydrogen chemisorbed during just-finished hydrogenation (there may have been different kinds of chemisorbed hydrogen), since it is suggested the molybdenum carbide is novel-metal-alike; thus is easy to absorb hydrogen. The HTPO profile of 2Mo/HMCM-22 after a 3-h reaction is interesting in that more than half of the cokes remained on the surface of the catalyst after hydrogenation. It is not difficult to explain: since molybdenum preferentially occupies the strongest acid sites of the zeolite, as has been verified by our NH_3-TPD (10) and pyridine-IR experiments (13), 2Mo/HMCM-22 catalyst will have the strongest acidity with respect to the other two catalysts. The stronger the acidity of the acid site is, the tighter the aromatic coke bonds to them. Thus, it makes hydrogenation of the aromatic carbonaceous depositions of the 2Mo/HMCM-22 catalyst more difficult compared with those of the other two catalysts. TPO and HTPO of 6Mo/HMCM-22 after a 6-h reaction are also shown in Fig. 7 (upper right corner). Besides the appearance of a tiny peak assigned to carbidic carbon at 573 K due to the removal of some molybdenum-associated coke (about 60% is removed in TPH), a sharp decrease in aromatic-type coke (about 90% is removed) is observed. Table 1 shows that after this kind of TPH, the activity of this catalyst is nearly fully restored. Some loss is probably due to the sublimation of molybdenum during these treatments. Therefore, the aromatic-type coke is suggested to be the key factor that leads to catalyst deactivation, since most of this kind of coke had been cleaned off and activity regenerated after TPH treatment. This is in good agreement with the large increase in catalyst stability with the addition of a small amount of CO to the reactant (pure methane) (21, 40). Under such situations, the irreversible coke (high-temperature peak) is greatly suppressed while the amount of Mo_2C-related coke is almost unchanged, which proves that these irreversible cokes are responsible for the short lifetime of the catalysts (22). On the other hand, it is less possible that molybdenum-associated coke is the species responsible for deactivation because, as mentioned several times, the formation of multilayered carbonaceous deposits on the molybdenum carbide surface does not hinder the activation of methane (11, 41), and the multilayered coke on the Mo center still exists after TPH and the restoration of catalyst activity. The mechanism for the deactivation of catalyst by aromatic-type coke has two aspects: site occupation and channel blockage. As shown by *in situ* proton NMR spectroscopy (42), the Brønsted acid site will react with the aromatics that stay on the zeolite surface (in TPO experiments, this is also a kind of carbonaceous deposits), leading to the disappearance of the 3.7 ppm peak in ^1H NMR spectra. If the charged species (such as $C_xH_{y+1}{}^{+1}$) can transform or leave the catalyst surface quickly and thus release the Brønsted proton, then the Brønsted proton will have the possibility of taking part in the transformation of new species, constituting a catalytic cycle. However when these carbonaceous species do not leave the Brønsted site,

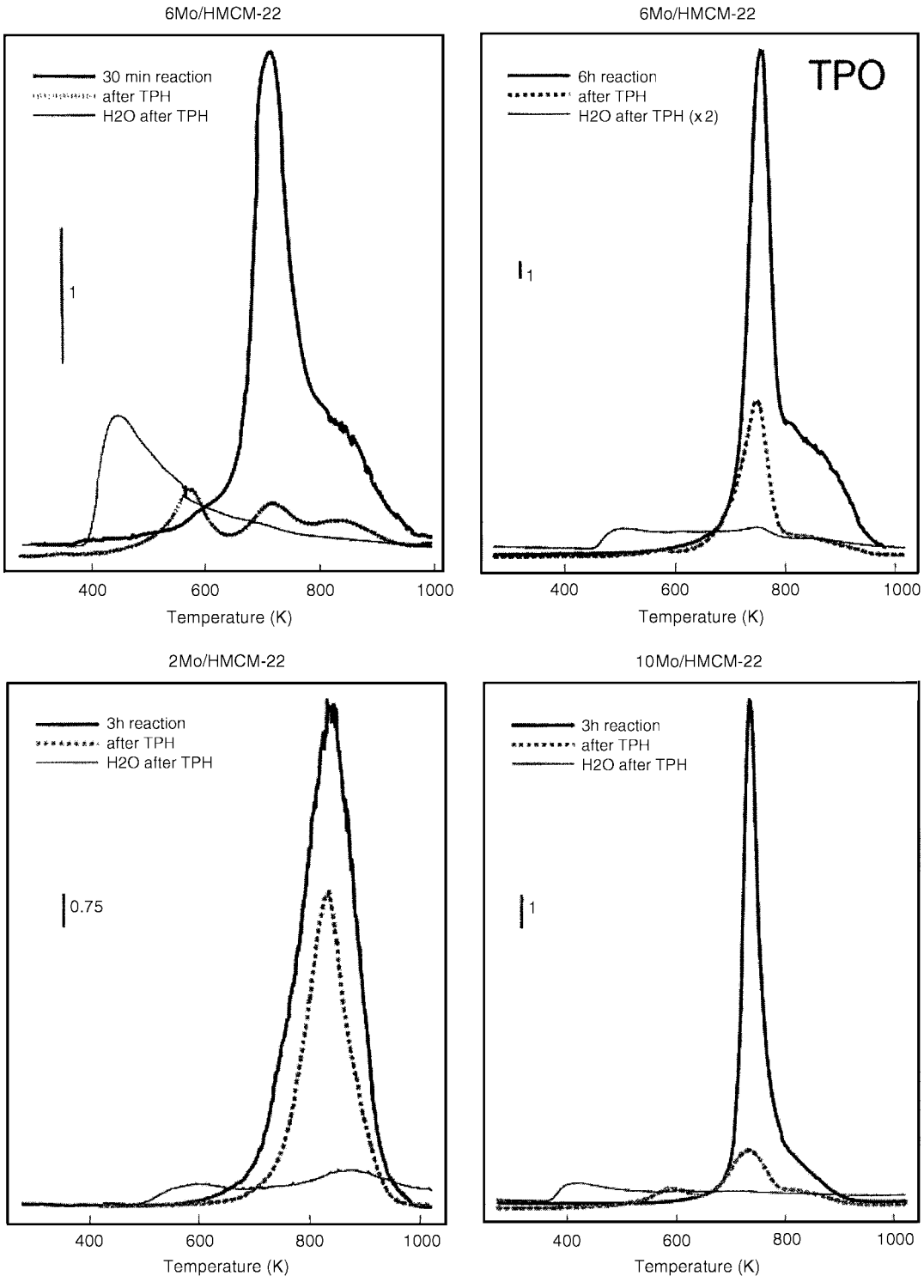

FIG. 7. TPO profiles of various catalysts before (thick line) and after (this line) TPH treatment (HTPO). The four curves are drawn to different scales. The hours of time on stream have been marked with a vertical line. For HTPO, the used catalysts first underwent a TPH treatment (with experimental conditions identical to that in Fig. 6), then were quenched in a H_2 flow to RT and swept by a pure He flow at the same temperature for 5 min. After further sweeping by a 10% O_2/He mixture (20 ml/min) at RT for 1 h, the HTPO experiments were begun from 303 to 1023 K with a heating rate of 8 K/min. The thin solid lines are the water production curves in HTPO experiments.

the Brønsted proton associated with them is unavailable for the transformation of new intermediates. Also, with further reaction, these irreversible cokes age and their sizes grow bigger, resulting in channel blockage and hence a decrease in the BET surface area of the catalysts, as discussed in the previous sections. Both these factors eventually lead to the deactivation of catalysts.

In summary, the types and amounts of carbonaceous deposits on the catalysts for methane aromatization is governed by the presence of different catalyst components and the relative amounts of these components. A totally different TPO profile can be seen when the ratio between the molybdenum species and the Brønsted acid sites is changed over a large range. The catalyst with the highest coke content is not the one with the worst catalytic performances. At least three kinds of carbonaceous deposits were observed in the oxidation of used 6Mo/HMCM-22 catalysts. They are carbidic carbon in molybdenum carbide (both from internal Mo ion and external Mo particles), molybdenum-associated coke, and (possibly) two aromatic-type cokes on acid sites. With time on stream, molybdenum carbide gets covered by molybdenum-associated coke, and the easily burned-off carbidic carbon is no longer visible in the TPO profiles. The content of molybdenum-associated coke grows bigger with reaction and reached C/Mo $\cong$ 9 after a 6-h reaction. A comparison of TPO and HTPO profiles of 6Mo/HMCM-22 after 6 h time on stream suggests that most of the aromatic-type cokes and part of the molybdenum-associated coke can be transformed into methane or ethene in TPH experiments. The activity of hydrogenated catalyst is nearly fully restored, which suggests that the aromatic-type cokes may be responsible for the deactivation of the catalyst.

ACKNOWLEDGMENTS

The authors thank the National Natural Science Foundation of China and the Ministry of Science and Technology of China for support. The kind donation of the mass spectrometer from the Alexander von Humboldt Foundation is gratefully acknowledged. The authors appreciate the reviewers' insightful comments and valuable suggestions. One of authors, DM, thanks Prof. S. T. Oyama for his helpful discussion.

REFERENCES

1. Sachtler, W. M. H., and Zhang, Z., *Adv. Catal.* **39**, 129 (1993).
2. Koningsberger, D. C., Degraaf, J., Mojet, B. L., Ramaker, D. E., and Miller, J. T., *Appl. Catal. A* **191**, 205 (2000).
3. Armor, J. N., *Microporous Mesoporous Mater.* **22**, 451 (1998).
4. Wang, L., Tan, L., Xie, M., Xu, G., Huang, J., and Xu, Y., *Catal. Lett.* **21**, 35 (1993).
5. Wang, D., Rosynek, M. P., and Lunsford, J. H., *J. Catal.* **169**, 347 (1997).
6. Solymosi, F., Cserenyi, J., Szoke, A., Bansagi, T., and Oszko, A., *J. Catal.* **165**, 150 (1997); Solymosi, F., Szoke, A., and Cserenyi, J., *Catal. Lett.* **39**, 157 (1996).
7. Liu, S., Wang, L., Ohnishi, R., and Ichikawa, M., *J. Catal.* **181**, 175 (1999).
8. Borry, R. W., III, Kim, Y. H., Huffsmith, A., Reimer, A., and Iglesia, I., *J. Phys. Chem. B* **103**, 5787 (1999).
9. Ma, D., Shu, Y., Bao, X., and Xu, Y., *J. Catal.* **189**, 314 (2000); Ma, D., Zhang, W., Shu, Y., Xu, Y., and Bao, X., *Catal. Lett.* **66**, 155 (2000).
10. Shu, Y., Ma, D., Bao, X., and Xu, Y., *Catal. Lett.* **70**, 67 (2000).
11. Ma, D., Shu Y., Cheng, M., Xu, Y., and Bao, X., *J. Catal.* **194**, 105 (2000).
12. Weckhuygen, B. M., Rosynek, M. P., and Lunsford, J. H., *Catal. Lett.* **52**, 31 (1998).
13. Ma, D., Wu, Z., Shu, Y., Zhou, D., Xu, Y., and Bao, X., submitted for publication.
14. Lerner, B. A., Zhang, Z., and Sachtler, W. M. H., *J. Chem. Soc. Fraday Trans.* **89**, 1799 (1993).
15. Fung, S. C., and Querini, C. A., *J. Catal.* **138**, 240 (1992).
16. Querini, C. A., and Fung, S. C., *J. Catal.* **141**, 389 (1993).
17. Querini, C. A., and Fung, S. C., *Appl. Catal. A* **117**, 53 (1994).
18. Goula, M. A., Lemonidou, A. A., and Efstathiou, A. M., *J. Catal.* **161**, 626 (1996).
19. Larsson, M., Jansson, J., and Asplund, S., *J. Catal.* **178**, 49 (1998).
20. Rubin, M., and Chu, P., U.S. Patent 4,954,325 (1990); Corma, A., Corell, C., and Pérez-Pariente, J., *Zeolites* **15**, 2 (1995).
21. Ames, W. F., "Numerical Methods for Partial Differential Equations," 2nd ed. Academic Press, New York, 1977.
22. Ohnishi, R., Liu, S., Dong, Q., Wang, L., and Ichikawa, M., *J. Catal.* **182**, 92 (1999).
23. Kim Y., Borry, R. W., III, and Iglesia, E., *Microporous Mesoporous Mater.* **35**, 495, (2000).
24. Wang, D., Rosynek, M. P., and Lunsford, J. H., *Top. Catal.* **3**, 289 (1996).
25. Li, W., Meitzner, G. D., Borry R. W., III, and Iglesia, E., *J. Catal.* **191**, 373 (2000).
26. Solymosi, F., Bugyi, L., Oszko, A., and Horvath, I., *J. Catal.* **185**, 160 (1999).
27. Meriaudeau, P., Ha, V. T. T., and Tiep, L. V., *Catal. Lett.* **64**, 49 (2000).
28. Meriaudeau, P., Tiep, L. V., Ha, V. T. T., Naccache, C., and Szabo, G., *J. Mol. Catal. A* **144**, 469 (1999).
29. Schuurman, Y., Decamp, T., Pantazidis, A., Xu, Y D., and Mirodatos, C., *Stud. Surf. Sci. Catal.* **109**, 351 (1997).
30. Haw, J. F., Goguen, P. W., Xu, T., Skloss, T. W., Song, W., and Wang, Z., *Angew. Chem.* **37**, 948 (1998).
31. Haw, J. F., Bicholas, J. B., Song, W., Deng, F., Wang, Z., Xu, T., and Heneghan, C. S., *J. Am. Chem. Soc.* **122**, 4763 (2000), and personal communication with one of the authors, Deng, F.
32. Kolodziejski, W., Zocovich-Wilson, C., Corell, C., Perez-Pariente, J., and Corma, A., *J. Phys. Chem.* **99**, 7002 (1995).
33. Lawton, S. L., Fung, A. S., Kennedy, G. J., Alemany, L. B., Chang, C. D., Hatzikos, G. H., Lissy, D. N., Rubin, M. K., Timken, H. C., Steuernagel, S., and Woessner, D. E., *J. Phys. Chem.* **100**, 3788 (1996).
34. Ma, D., Shu, Y., Han, X., Liu, X., Xu, Y., and Bao, X., *J. Phys. Chem. B* **105**, 1786 (2001).
35. Corma, A., Corell, C., Fornes, V., Kolodziejski, W., and Perez-Pariente, J., *Zeolites* **15**, 576 (1995).
36. Ding, W., Li, S., Meitzner, G. D., and Iglesia, E., *J. Phys. Chem. B* **105**, 506 (2001).
37. Guisnet, M., and Magnoux, P., *Stud. Surf. Sci. Catal.* **88**, 53 (1994); Hnadreck, G. P., and Smith, T. D., *J. Catal.* **123**, 513 (1990).
38. Leonowicz, M. E., Lawton, J. A., Lawton, S. L., and Rubin, M. K., *Science* **264**, 1910 (1994).
39. Guczi, L., van Santen, R. A., and Sarma, K. V., *Catal. Rev.–Sci. Eng.* **38**, 249 (1996).
40. Liu, S., Dong, Q., Ohnishi, R., and Ichikawa, M., *J. Chem. Soc. Chem. Commun.* 1217 (1998).
41. Miyao, T., Shishikura, I., Matsuoka, M., Nagai, M., and Oyama, S. T., *Appl. Catal. A* **165**, 419 (1997).
42. Ma, D., Shu, Y., Zhang, W., Han, X., Xu, Y., and Bao, X., *Angew. Chem.* **39**, 2928 (2000).